vol. 175, no. 3 the american naturalist march 2010

E-Article

The Independent and Interactive Effects of Tree-Tree Establishment Competition and Fire on Savanna Structure and Dynamics

Justin M. Calabrese,[1,*] Federico Vazquez,[2] Cristóbal López,[2] Maxi San Miguel,[2] and Volker Grimm[1]

1. Department of Ecological Modelling, Helmholtz Centre for Environmental Research (UFZ), Permoserstrasse 15, 04318 Leipzig, Germany; 2. Instituto de Física Interdisciplinar y Sistemas Complejos (Consejo Superior de Investigaciones Científicas–Universitat de les Illes Balears), E-07122 Palma de Mallorca, Spain

Submitted January 13, 2009; Accepted September 1, 2009; Electronically published January 25, 2010

abstract: Savanna ecosystems are widespread and economically important and harbor considerable biodiversity. Despite extensive study, the mechanisms regulating savanna tree populations are not well understood. Recent empirical work suggests that both tree-tree competition and fire are key factors in semiarid to mesic savannas, but the potential for competition to structure savannas, particularly in interaction with fire, has received little theoretical attention. We develop a minimalistic and analytically tractable stochastic cellular automaton to study the individual and combined effects of these two factors on savannas. We find that while competition often substantially depresses tree density, fire generally has little effect but can drive tree extinction in extreme scenarios. When combined, competition and fire interact nonlinearly with strong negative consequences for tree density. This novel result may help explain observed variability among apparently similar savannas in their response to fire. Paradoxically, this interaction could also render the presence of competition more difficult to detect in empirical studies because fire can override the characteristic regular spacing driven by competition and lead instead to clustering.

Keywords: establishment, grass-dependent fire, mean-field approximation, nonlinear interaction, pair approximation, spatially explicit model.

Introduction

Savannas are widespread and important ecosystems that are characterized by a persistent mixture of trees and grasses and occur across a broad range of climatic, edaphic, and ecological conditions (Scholes and Archer 1997; Sankaran et al. 2005). Research on savannas has focused intensely on the so-called savanna problem: what is unique about savannas that allows the continual coexistence of trees and grasses where in other biomes one or the other growth form dominates (Sarmiento 1984)?

Attempts to address the savanna problem theoretically have tended to range between two extremes. On the one hand, much research has focused on single-factor explanations, such as how rooting-depth separation mediates tree-grass competition for water (Walker et al. 1981; Walker and Noy-Meir 1982) or how fire promotes coexistence by constraining tree density (D'Odorico et al. 2006; Hanan et al. 2008). On the other hand, many studies have incorporated a wide range of factors thought to be important, many of which may be site specific (Menaut et al. 1990; Jeltsch et al. 1996; Higgins et al. 2000; Baxter and Getz 2005). While it is clear that single-factor explanations are oversimplified and inadequate (Bond 2008), it is also apparent that complicated, site-specific models of savanna dynamics will likely not provide general and robust answers. Instead, studies that focus on a small number of key factors and their interactions are needed to tease apart the savanna problem (e.g., Hochberg et al. 1994; Scheiter and Higgins 2007; Sankaran et al. 2008; Holdo et al. 2009). This general approach has proved successful in understanding a wide range of ecological systems (Grimm et al. 2005).

Recent large-scale analyses of the determinants of tree cover in African savannas have found that mean annual precipitation (MAP) is a strong constraint in arid to mesic savannas (<650 mm MAP), while in semiarid to humid savannas, fire is often important (Bond et al. 2003; Sankaran et al. 2005, 2008; Bucini and Hanan 2007; Bond 2008). These findings suggest that in semiarid to mesic savannas, both water limitation and fire may play important roles in structuring tree populations and, as we describe below, may have the potential to interact in counterintuitive ways. We discuss each factor in turn.

Savanna trees often have root systems that extend lat-

* Corresponding author; e-mail: justin.calabrese@ufz.de.

Am. Nat. 2010. Vol. 175, pp. E44–E65.
DOI: 10.1086/650368

erally well beyond their crowns (Belsky 1994; Scholes and Archer 1997; Schenk and Jackson 2002; Casper et al. 2003). Coupling this fact with the above-mentioned water limitation suggests that trees might negatively influence their neighbors via belowground competition for water. In particular, the asymmetric negative effects of adult trees with extensive root networks on nearby seedlings and saplings, which we refer to as "establishment competition," could limit tree density (Pellew 1983; Barot et al. 1999; Jeltsch et al. 2000; Wiegand et al. 2006). Although tree-tree competition has received less research attention than tree-grass competition, empirical evidence for its effects on tree density and spatial structure has been accumulating in the savanna literature, particularly in sites with <650 mm MAP (table 1).

The study of tree-tree competition is complicated by observations that local facilitation among trees may sometimes be important (Scanlon et al. 2007). Facilitation can occur when trees improve local nutrient or water conditions, but this form of facilitation typically operates only below tree crowns (Belsky et al. 1989, 1993). Longer-distance facilitation may arise from other causes, such as dispersal patterns (Barot et al. 1999; Scanlon et al. 2007). For example, dispersal-mediated local facilitation could result from either true dispersal limitation (most seeds end up near the parent tree) or an "island of fertility" effect (Scholes and Archer 1997). In the latter case, trees attract seed-dispersing animals such that seeds tend to be deposited near trees. Although the role of dispersal limitation in savannas is not fully resolved, it seems likely that there will be some tendency for elevated tree seed densities near trees (Gutiérrez and Fuentes 1979; Tybirk et al. 1994; Barot et al. 1999; Witkowski and Garner 2000), which would tend to promote clumped tree distributions and might interact with local competitive processes.

Fire, which negatively affects immature trees yet to escape the flame zone, has received increasing recognition for its role in structuring savannas (Higgins et al. 2000; Peterson and Reich 2001). In addition to large-scale empirical evidence of the importance of fire (Bond et al. 2003; Sankaran et al. 2005; Bucini and Hanan 2007; Bond 2008), recent spatially implicit analytical models have highlighted its ability to induce multiple stable states in savanna systems (van Langevelde et al. 2003; D'Odorico et al. 2006; Hanan et al. 2008). These studies have demonstrated that a positive feedback cycle can develop whereby increasing grass biomass leads to more frequent and intense fires, which in turn negatively affect trees, leading to higher grass biomass, and so on. Thus, under some conditions, fire may exert a strong influence on tree density. Furthermore, fire has been also been observed to promote tree clustering (Barot et al. 1999; Kennedy and Potgieter 2003), but the conditions under which this can occur are not fully understood.

Because tree-tree competition and fire can both target the same, vulnerable tree life stage, they could exert particularly strong combined effects on tree density. Furthermore, as these two factors may influence spatial patterning in opposite directions and on different scales, it is not clear when and over which scales clustering will dominate relative to regular dispersion and vice versa. This is especially true when local dispersal-mediated facilitation, which will tend to promote clustering, is also operating. Despite increasing empirical support for the importance of competition and fire, most theoretical studies have ignored one (usually competition) or both of them. The studies incorporating both factors are complex, rule-based simulation models that simultaneously include many other processes (Menaut et al. 1990; Jeltsch et al. 1996, 1998, 1999; Baxter and Getz 2005; Meyer et al. 2007). Although such models can often reproduce observed patterns (e.g., Jeltsch et al. 1999), their complexity makes pinpointing exactly what is driving the pattern formation difficult, even after extensive analysis. Therefore, the role that establishment competition might play in constraining tree abundance and shaping tree spatial distribution, particularly when it interacts with fire and dispersal-mediated facilitation, remains unclear.

Here, we explore the individual and combined effects of establishment competition and grass-dependent fire on

Table 1: Empirical examples demonstrating competition among savanna trees

Region/location	MAP (mm)	Source
Khomas Hochland, Namibia	100–200	Wiegand et al. 2006
Kalahari Gemsbok National Park, South Africa	209–220	Jeltsch et al. 1999
Kalahari, Botswana	300	Skarpe 1991
Central Valley, Chile	356–449	Gutiérrez and Fuentes 1979
Kalahari, South Africa	377	Meyer et al. 2008
Kalahari, South Africa	411	Moustakas et al. 2006, 2008
Mkuzi Game Reserve, South Africa	610	Smith and Goodman 1986
Nylsvley Provincial Nature Reserve, South Africa	630	Smith and Grant 1986
Lamto Research Station, Ivory Coast	1,300	Barot et al. 1999

Note: MAP = mean annual precipitation.

savanna structure. We develop a minimalistic, spatially explicit, and stochastic cellular automaton that exploits the middle ground between highly detailed but difficult-to-analyze savanna simulation models and analytically tractable but spatially implicit aggregated models. A key strength of our approach is that, by using mean-field and pair approximations (Matsuda et al. 1992; Ellner 2001), we can establish analytically the conditions under which the model's important qualitative transitions occur.

Material and Methods

The model, which is an extension of the contact process (Marro and Dickman 1999), is implemented as a continuous-time, discrete-state Markov chain on a square lattice with periodic boundary conditions. Each lattice site is in either state 1 (tree) or state 0 (grass). The proportion of tree-occupied sites on the lattice is denoted $\rho[1]$, and the proportion of grass-occupied sites is $\rho[0] = 1 - \rho[1]$. We assume that each site is 5 m × 5 m and model a lattice of size of $L = 200$ sites per side, for a total area of 100 ha.

In the manner of other demographic savanna models, we assume that the major bottleneck in tree life histories is the set of transitions from seed to adult (Higgins et al. 2000; Sankaran et al. 2004). To maintain tractability, we lump these into a single transition (establishment) and assume, as we are interested in the long-term dynamics of the tree populations, that this transition is effectively instantaneous. Given that a seed is dispersed to a grass-occupied site, establishment depends only on the new tree's chances of surviving both competition and fire.

Interaction Neighborhoods

Dispersal (facilitation) and competition (negative facilitation) are spatially limited and thus require the definition of the neighborhoods over which they operate. We use Moore neighborhoods and define the "near" neighborhood to be the $z_n = 8$ sites immediately surrounding the focal site and the "far" neighborhood as the $z_f = 16$ sites surrounding the near neighborhood. The dispersal and competition neighborhoods are defined below on the basis of these building blocks.

Death

A site in state 1 transitions to state 0 at a constant rate α, independent of the status of its neighbors. As is customary in similar cellular automata models, we set, without loss of generality, $\alpha = 1$. This amounts to an implicit rescaling of time such that time now proceeds in units of average tree life span ($1/\alpha$).

Birth/Dispersal

The lateral extension of roots defines the spatial scale over which trees can exert a competitive influence on their neighbors. In contrast, although seeds may tend to be deposited near trees, there is no hard upper limit on dispersal distance. We therefore assume that the spatial scale of dispersal is generally greater than that of competition, and thus the dispersal neighborhood comprises both the near and far neighborhoods. Each site within the dispersal neighborhood of a tree receives seeds at rate $\beta = b/(z_n + z_f)$ independent of its occupancy status, where b is the per tree birth rate. If a seed lands on a tree-occupied site, nothing happens. If it lands on a grass-occupied site, it has a chance to establish as an adult tree.

Establishment

A seed that has landed in a grass-occupied site can establish (instantaneously) in that site if it survives both competition (with probability P_C^{Surv}) with nearby adult trees and fire (with probability P_F^{Surv}). Thus, the probability of establishment is $P_E = P_C^{Surv} P_F^{Surv}$.

Competition with Adult Trees. The spatial scale of establishment competition is defined by the competition neighborhood, which we set equal to the near neighborhood defined above. Given that a seed has landed in a grass-occupied site, the probability that it establishes decreases exponentially with the number of competitors, $P_C^{Surv} = e^{-\delta S}$, where S is the number of trees in the competition neighborhood and δ is a coefficient scaling the intensity of competition. Note that the total effect of competition, P_C^{Surv}, is a function of both neighborhood density (S) and competition intensity (δ). When we refer to the intensity or strength of competition, we are referring specifically to the value of the competition parameter δ. In addition to the above-described establishment competition, there is also preemptive competition for sites in our model, in the sense that once a tree occupies a site, it cannot be displaced by a new tree (Hochberg et al. 1994). Hereafter, when we refer to competition, we mean establishment competition and not preemptive site competition. Finally, we note that Bolker et al. (2000) studied a similar, generic model of plant competition but did not include the effects of fire.

Fire. The occurrence of fire in savannas depends strongly on grass biomass, and fires are generally larger than the 100-ha lattice modeled here (van Wilgen et al. 2000). Furthermore, fire influences savanna tree populations primarily by inhibiting the transition from the juvenile (fire-sensitive) to the adult (fire-resistant) life stages (Peterson and Reich 2001; Hanan et al. 2008). The precise mecha-

nisms by which fire exerts its effects are complex and not fully understood (Scholes and Archer 1997). To maintain tractability, we therefore take a phenomenological approach and model only the probability of a juvenile tree ultimately surviving fire. In doing so, we ignore complications that may be important in some savannas, such as juvenile trees persistently resprouting after being top-killed by fire (Boaler and Sciwale 1966; Holdo 2005, 2006; Neke et al. 2006) and spatial correlations in the effects of fire (van Wilgen et al. 2000). To our knowledge, such mechanisms have been incorporated only in considerably more detailed savanna models (e.g., Pellew 1983; Menaut et al. 1990; Higgins et al. 2000; Holdo et al. 2009).

We assume that the probability of a killing fire occurring while an individual is trying to establish is a Michaelis-Menten (saturating) function of grass biomass, which is similar to the implementation of fire in Jeltsch et al. (1996). The per-birth probability of surviving fire is, then,

$$P_{\mathrm{F}}^{\mathrm{Surv}} = 1 - \frac{\gamma k(1 - \rho[1])}{\tilde{\sigma} + k(1 - \rho[1])}, \tag{1}$$

where k is a constant that converts grass cover to grass biomass; γ, which we set to 1 for the following analyses, is the asymptotic (maximum) probability of fire occurrence as grass biomass goes to infinity; and $\tilde{\sigma}$ is the grass biomass at which the probability of fire reaches half its maximum value. Defining $\sigma = \tilde{\sigma}/k$, the probability of surviving fire can be written

$$P_{\mathrm{F}}^{\mathrm{Surv}} = \frac{\sigma}{\sigma + 1 - \rho[1]}. \tag{2}$$

Given this parameterization, we see that the negative effects of fire increase with decreasing σ.

The model thus described has three free parameters: the per-tree birth rate b, the competition parameter δ, and the fire parameter σ. In the following, we focus mainly on how δ and σ affect tree density and spatial pattern. A description of the algorithm used to simulate the model and the source code can be found in appendix A.

Analytical Approximations

It is possible to find deterministic differential equations that describe approximately the time evolution of the above-defined stochastic model. We consider two levels of description: a mean-field approximation (MFA), where only the global behavior of tree density is considered, and a multiscale pair approximation (MSPA; Ellner 2001), which accounts for the spatial dependence of the mean density. Detailed derivations of both approximations, following Ellner (2001), are provided in appendix B. Here, we present the approximations and highlight the distinction between them.

Both approximations are based on using the transition rules of the simulation model to find an equation for the dynamics of the mean tree density, $\rho[1]$, in terms of different kinds of site frequencies. The singlet frequency, $\rho[i]$, is the global unconditional probability of sites being in state i. Pair frequencies, $\rho[ij]$, give the probability that a randomly selected site is in state i and a randomly selected neighboring site is in state j. Conditional pair frequencies, $q[j|i]$, are the conditional probabilities that a neighboring site is in state j, given that the focal site is in state i. The dynamics of the mean density of trees can then be expressed as (app. B)

$$\frac{d\rho[1]}{dt} = \beta(z_{\mathrm{n}}q_{\mathrm{n}}[1|0] + z_{\mathrm{f}}q_{\mathrm{f}}[1|0])e^{-\delta z_{\mathrm{n}}q_{\mathrm{n}}[1|0]} \times \frac{\sigma}{\sigma + 1 - \rho[1]}(1 - \rho[1]) - \rho[1], \tag{3}$$

where $q_{\mathrm{n}}[1|0]$ and $q_{\mathrm{f}}[1|0]$ are the expected local densities of tree-occupied sites around a site in state 0 in the near and far neighborhoods, respectively. Equation (3) is the starting point for the mathematical modeling of the system, with the MFA approximating it and the MSPA extending it.

In the MFA, we ignore the spatial correlations that build up in the simulation model by replacing the conditional local density terms with the unconditional global site occupancy probability $\rho[1]$. This yields a closed equation for mean tree density,

$$\frac{d\rho[1]}{dt} = \beta(z_{\mathrm{n}}\rho[1] + z_{\mathrm{f}}\rho[1])e^{-\delta z_{\mathrm{n}}\rho[1]} \times \frac{\sigma}{\sigma + 1 - \rho[1]}(1 - \rho[1]) - \rho[1], \tag{4}$$

which is intentionally written to emphasize the differences with respect to equation (3). Given that we are interested in the long-time behavior of $\rho[1]$, we focus in the next section on the stationary solutions of equation (4).

The MSPA is obtained by first writing the conditional local densities in terms of singlet and pair frequencies and then using the rules of the simulation model to write equations for the pair frequencies in the near ($\rho_{\mathrm{n}}[11]$) and far ($\rho_{\mathrm{f}}[11]$) neighborhoods. This yields the coupled, closed system (app. B)

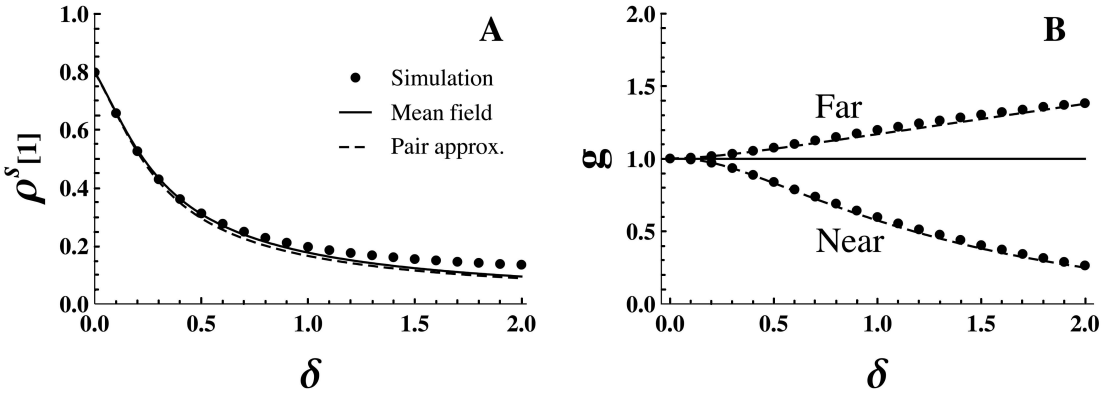

Figure 1: Individual effects of competition on stationary tree density ($\rho^s[1]$; *A*) and near- and far-neighborhood spatial pattern (g; *B*) for the no-fire ($\sigma = \infty$) case. Points represent the means of 100 samples from a simulation after it had reached its stationary state. Solid and dashed lines are obtained by numerically integrating the mean-field approximation (MFA) and the multiscale pair approximation (MSPA), respectively. *A* shows the strong negative effect of competition on stationary tree density, with even slight competition leading to a substantial reduction in $\rho^s[1]$. *B* shows the corresponding spatial pattern as a function of competition, with increasingly regular dispersion observed in the near neighborhood ($g_n < 1$) and increasingly clumped distributions in the far neighborhood ($g_f > 1$). Both the MFA and the MSPA agree reasonably well with the simulation with respect to $\rho^s[1]$ (*A*), but only the MSPA (*B*) captures the spatial pattern that develops in the simulation.

$$\frac{d\rho[1]}{dt} = \beta(z_n q_n[1|0] + z_f q_f[1|0])e^{-\delta z_n q_n[1|0]} \times \frac{\sigma}{\sigma + 1 - \rho[1]}(1 - \rho[1]) - \rho[1], \quad (5a)$$

$$\frac{1}{2}\frac{d\rho_n[11]}{dt} = \beta[1 + (z_n - 1)q_n[1|0] + z_f q_f[1|0]]e^{-\delta(1+[z_n-1]q_n[1|0])} \times \frac{\sigma}{\sigma + 1 - \rho[1]}(\rho[1] - \rho_n[11]) - \rho_n[11], \quad (5b)$$

$$\frac{1}{2}\frac{d\rho_f[11]}{dt} = \beta[z_n q_n[1|0] + 1 + (z_f - 1)q_f[1|0]] \times e^{-\delta z_n q_n[1|0]} \times \frac{\sigma}{\sigma + 1 - \rho[1]}(\rho[1] - \rho_f[11]) - \rho_f[11], \quad (5c)$$

where $q_n[1|0] = (\rho[1] - \rho_n[11])/(1 - \rho[1])$ and $q_f[1|0] = (\rho[1] - \rho_f[11])/(1 - \rho[1])$.

Each pair frequency is, when divided by tree density squared, the normalized pair correlation statistic, g, widely used in spatial statistics (Stoyan and Stoyan 1994; Wiegand and Moloney 2004). The normalized g statistic equals 1 for a random spatial distribution, with values greater and less than 1 indicating clustered and regular distributions, respectively. In continuous space, g is a continuous function of distance, but in the lattice case treated here, g proceeds by discrete neighborhoods. Thus, we define the normalized pair correlation statistic for the near and far neighborhoods, respectively, as

$$g_n = \frac{\rho_n[11]}{\rho^2[1]}, \qquad g_f = \frac{\rho_f[11]}{\rho^2[1]}. \quad (6)$$

As there are no spatial processes in the model acting beyond the far neighborhood, the g statistic for neighborhoods three cells away and farther, g_{3+}, in the MSPA equals 1 (app. B). Thus, with g_n, g_f, and g_{3+}, we have a direct link between variation in model parameters and scale-dependent tree spatial pattern.

Results

For a given set of parameters (b, δ, and σ) and a random initial condition, $\rho[1]$, $\rho_n[11]$, and $\rho_f[11]$ reach the stationary values $\rho^s[1]$, $\rho^s_n[11]$, and $\rho^s_f[11]$ after a short transient period. We obtained a rough estimate of the tree birth rate b by noting that the empirically observed upper limit of savanna tree cover across African savannas is approximately 0.8 at intermediate to high MAP (Sankaran et al. 2005; Bucini and Hanan 2007). At such levels of MAP, water is no longer limiting, which in our framework translates into no competition ($\delta = 0$). For this upper limit to be realized, disturbances must also be absent, implying no fire ($\sigma = \infty$). The MFA is quantitatively accurate in this no-competition, no-fire limit (fig. 1*A*), and in the time-

rescaled model ($\alpha = 1$), its stationary solution (app. C) depends only on b:

$$\rho^{s}[1] = \frac{b-1}{b}. \tag{7}$$

Setting $\rho^{s}[1] = 0.8$ and solving for b yields $b = 5$.

As we are primarily interested in the abilities of competition and fire to limit tree density and shape tree spatial pattern, we simulated the above-described model for $b = 5$ and various values of the parameters δ and σ. In appendix D, we present an additional set of figures analogous to those below but for the case $b = 8$. In general, the accuracy of our approximations depends on b and will decrease as b nears the lower threshold for tree persistence (Ellner 2001). In appendix B, we discuss how and why the accuracy of the approximations is also affected by the strength of competition.

In the absence of fire ($\sigma = \infty$), increasing competition strength (δ) in the simulation causes tree density to approach a lower limit of $\rho^{s}[1] \approx 0.1095$. Importantly, even relatively weak competition can have a sizable quantitative influence on tree density (fig. 1*A*). Correspondence between the simulations and both the MFA and the MSPA is generally good for $\rho^{s}[1]$ and the spatial-pattern indices (g_n and g_f), but it begins to break down as competition strength increases (fig. 1). Strong establishment competition quickly overcomes the tendency toward clustering caused by dispersal limitation and leads to increasingly regular distributions at the near-neighborhood scale ($g_n < 1$), while the far neighborhood becomes increasingly clustered ($g_f > 1$; fig. 1*B*). The MFA and the MSPA differ only slightly in $\rho^{s}[1]$ when competition is very strong, suggesting that for practical purposes, the clear, nonrandom spatial pattern that develops does not feed back strongly on mean tree density.

When there is no competition ($\delta = 0$), fire has only a slight effect on $\rho^{s}[1]$ for most of the range of σ values (fig. 2). The weak influence of fire when it is infrequent (intermediate to large σ) contrasts sharply with its effects when σ decreases toward a critical value σ_c (fig. 2). When $\sigma \leq \sigma_c$, the strong, negative effect of frequent fire on tree establishment drives the tree population to extinction ($\rho^{s}[1] = 0$). Because of the close correspondence between the MFA and the MSPA, we can use the simpler MFA to further analyze this transition. In appendix C, we obtain from the MFA the stationary solution for $\rho[1]$ when both $\rho[1]$ and δ are small:

$$\rho^{s}[1] = \frac{1 + (1-b)\sigma}{1 - b\sigma(1 + \delta z_n)}. \tag{8}$$

A better, though more complicated, approximation of $\rho^{s}[1]$ is also possible for arbitrary $\rho[1]$ and is shown in appendix C. From equation (8), $\rho[1]$ becomes 0 when σ takes the value

$$\sigma_c = \frac{1}{b-1}. \tag{9}$$

Note that under the MFA, this transition from tree-grass coexistence to a grass-only state is independent of δ and is driven only, for a fixed value of the birth rate, by σ. This can be seen in figure 2, where for the deterministic approximations, $\rho^{s}[1] = 0$ when $\sigma = \sigma_c$, regardless of the level of competition. However, because of stochastic finite-size fluctuations ignored by the deterministic approximations, σ_c in the simulations is always larger than that given by equation (9) (Stanley 1971), and this discrepancy increases with the strength of competition (fig. 2).

As can be seen in figure 2, fire acting independently has relatively little effect on equilibrium tree abundance until it becomes quite frequent (i.e., σ near σ_c), whereas figure 1 shows that competition acting alone has pronounced effects on $\rho^{s}[1]$. Combining fire with competition produces, as expected, a further decrease in $\rho^{s}[1]$. However, the magnitude of the decrease in $\rho^{s}[1]$ resulting from the

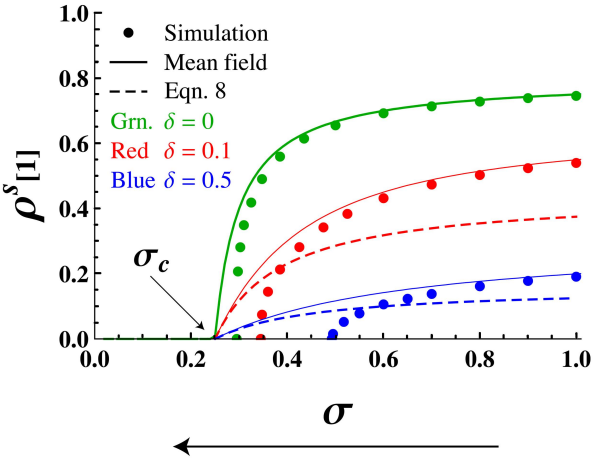

Figure 2: Effects of fire on stationary tree density $\rho^{s}[1]$ with and without competition. Colors refer to the competition intensity (*green*, $\delta = 0$; *red*, $\delta = 0.1$; and *blue*, $\delta = 0.5$). Points represent the means of 100 samples from a simulation after it had reached its stationary state. The solid lines are obtained by numerically integrating the mean-field approximation, while dashed lines are from equation (8). The arrow along the *X*-axis indicates that fire frequency increases as σ decreases. Fire tends to have little effect on $\rho^{s}[1]$, but as σ approaches σ_c (eq. [9]), the negative effect of fire strongly depresses $\rho^{s}[1]$. When $\sigma \leq \sigma_c$, fire drives the tree population extinct. Although competition does not affect σ_c in the deterministic approximations, the deviation between equation (9) and the value of σ_c estimated from the simulations increases with competition strength.

addition of fire depends nonlinearly on the strength of competition (fig. 3). In other words, adding fire to the competition curve in figure 1*A* changes the curve's shape rather than simply shifting it downward by a constant amount. This can be seen more clearly by plotting the difference in stationary tree density, $\Delta\rho^s[1] = \rho^s_{\sigma=\infty}[1] - \rho^s_{\sigma<\infty}[1]$, between the case where competition acts alone ($\sigma = \infty$) and each case where competition and fire act together (fig. 3). The $\Delta\rho^s[1]$ curve represents the additional reduction of $\rho^s[1]$ when fire and competition are combined relative to when competition acts alone. From figure 3, we see that the $\Delta\rho^s[1]$ curve peaks at small to intermediate values of δ, meaning that fire will have its greatest effects when competition intensity is relatively low. In appendix C, we derive, from equation (8), an analytical approximation for this difference and use it to show that an interior peak at low to intermediate δ is a general feature of the $\Delta\rho^s[1]$ curve.

We now focus on using the g statistics derived from the MSPA to analyze how competition and fire shape spatial pattern in the model. As we demonstrate below, the qualitative transitions in spatial patterning tend to occur when σ is near σ_c. However, in figure 2 we showed that the analytical approximations and the simulations can differ substantially in σ_c when competition is operating. This difference in σ_c results in a discrepancy between the g statistics calculated directly from the simulations and those derived from the MSPA, the magnitude of which increases with competition strength. To correct for this discrepancy, we introduce $\hat{\sigma} = \sigma - \sigma_c$, a shifted fire parameter that is now independent of σ_c and allows direct comparison between the simulation and MSPA results (Stanley 1971). All results below are expressed in terms of $\hat{\sigma}$.

Figure 4 shows lattice snapshots together with their corresponding g statistic values where increasing fire frequency (decreasing $\hat{\sigma}$) drives a transition from regular ($g_n < 1$; fig. 4*A*) to random ($g_n = 1$; fig. 4*B*) and then to clumped ($g_n > 1$; fig. 4*C*) tree dispersion at the near-neighborhood scale. In contrast, tree spatial distributions are persistently clumped at the far-neighborhood scale ($g_f > 1$) and clumped or approximately random at larger distances ($g_{3+} \geq 1$; fig. 4). To better understand the near-neighborhood transitions, we hold b constant and focus on how the interplay between competition and fire shapes spatial pattern. In figure 5, the $g_n = 1$ lines separate the $(\hat{\sigma}, \delta)$ plane into regions where local clumping and regular dispersion occur. Increasingly frequent fire (small $\hat{\sigma}$) can drive a transition from the regular spacing promoted by competition to clustering, even when competition is very strong (large δ; fig. 5). In appendix C, we obtain an analytical approximation for this pattern transition ($g_n = 1$) line,

$$\hat{\sigma}(\delta) = \frac{\sigma_c m(1 + bz_n\delta)}{bzme^{\delta} + z_n + \delta + z(z + \delta - me^{\delta}) - b\{z^2 + z_n + m[1 + \delta(1 + z_n)]\}}, \tag{10}$$

where we have defined $z = z_n + z_f$ and $m = z + 1$. Equation (10) allows one to quickly assess how variation in model parameters influences near-neighborhood spatial

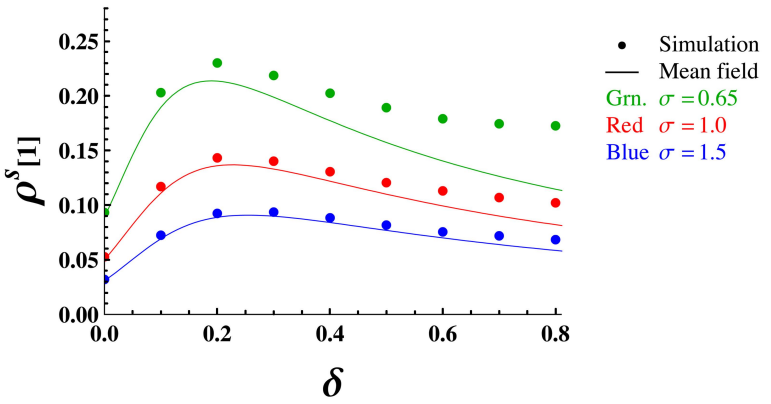

Figure 3: Nonlinear effects of competition and fire on stationary tree density. Colors refer to the level of fire (*green*, high fire [$\sigma = 0.65$]; *red*, medium fire [$\sigma = 1.0$]; *blue*, low fire [$\sigma = 1.5$]), points represent means from simulations, and solid lines are from the mean-field approximation (MFA). In general, the magnitude of the additional effect of fire on tree density ($\Delta\rho^s[1]$) depends on the level of competition. The MFA captures this qualitative result well and suggests that the maximum effect of a given amount of fire will occur when fire is combined with weak to intermediate competition.

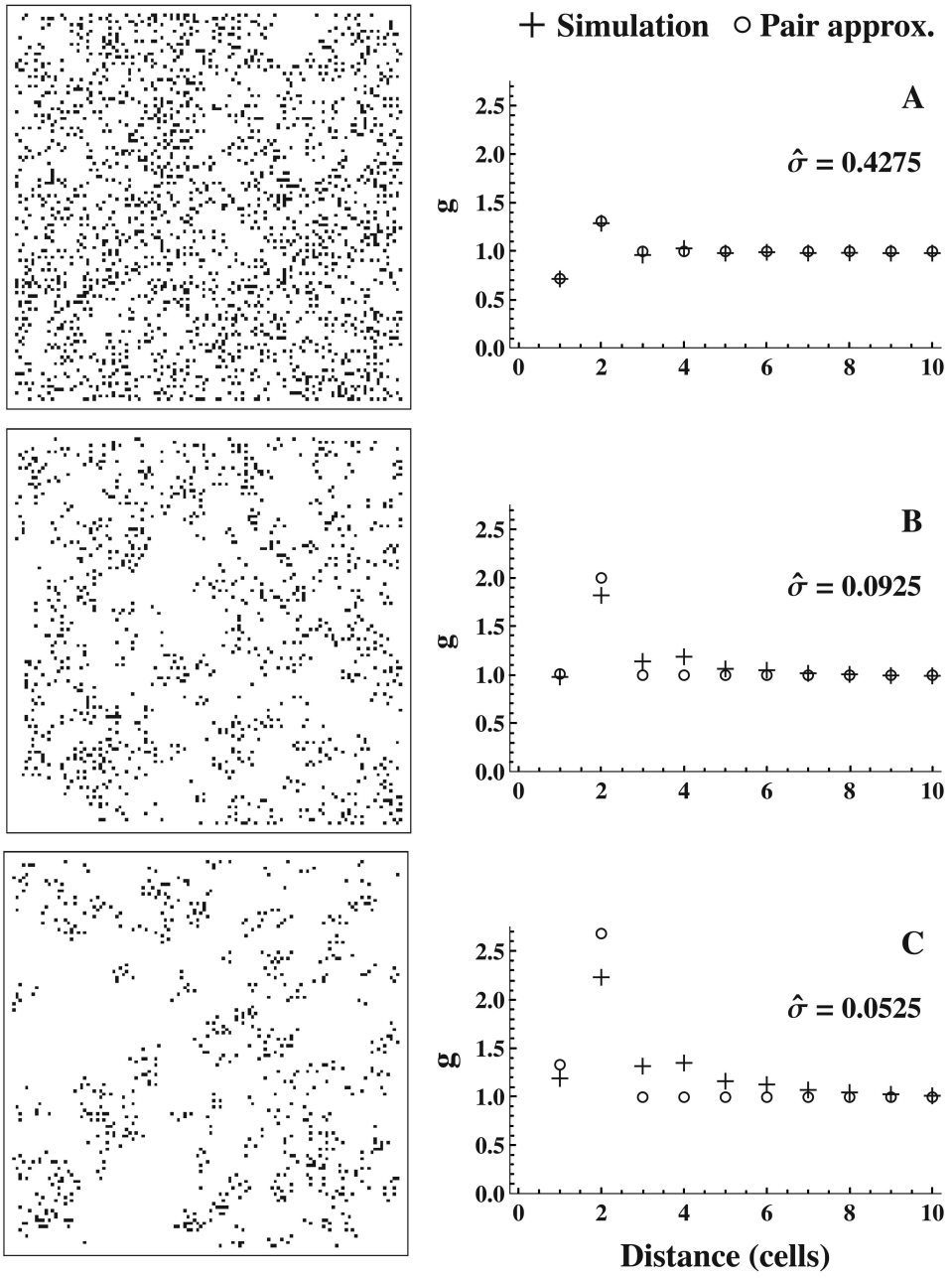

Figure 4: Distance-dependent spatial pattern under three different values of the shifted fire parameter $\hat{\sigma}$ ($b = 5, \delta = 0.75$ for all panels). The left column shows a single snapshot of the central 120 × 120-cell area of a 200 × 200 lattice well after the simulation had reached its stationary state. Black cells are tree occupied, and white cells are grass occupied. The corresponding plot to the right of each lattice picture shows the mean value of the g statistic as a function of distance (*plus signs*), calculated from 100 samples of the lattice taken after the simulation had reached stationary state. The circles represent the corresponding g statistics calculated from the multiscale pair approximation (MSPA). At distances of three cells and farther (g_{3+}), the MSPA predicts a random spatial pattern. Tree spatial-pattern transitions from regular ($\hat{\sigma} = 0.4275$, $g_n < 1$; *A*) to random ($\hat{\sigma} = 0.0925$, $g_n = 1$; *B*) and then to clustered ($\hat{\sigma} = 0.0525$, $g_n > 1$; *C*) at the near-neighborhood scale as fire frequency increases. Trees are persistently clumped at the far-neighborhood scale and random to clumped at larger distances. The MSPA describes the near- and far-neighborhood spatial patterns well but fails to account for the increasing clustering at the g_{3+} scale as fire frequency increases.

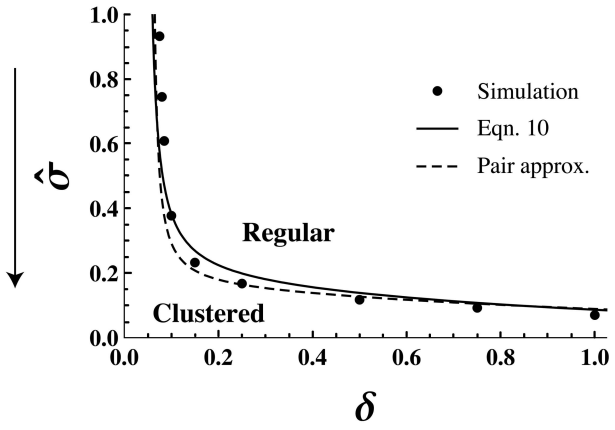

Figure 5: Near-neighborhood spatial pattern in the $(\hat{\sigma}, \delta)$ plane for $b = 5$, showing two distinct tree-spacing regions. The solid line, the dashed line, and the circles represent different versions (from eq. [10], the multiscale pair approximation [MSPA], and the simulations, respectively) of the pattern transition line ($g_n = 1$) that separates regions of clustering ($g_n > 1$) and regular spacing ($g_n < 1$). A numerical search was used to find the point at which $g_n \approx 1$ for each value of δ in both the MSPA and the simulations. In the case of the simulations, the mean g_n (*circles*) was calculated from 100 samples from a simulation that had reached stationary state, and adaptive spacing of points along the *X*-axis was used to reach an appropriate compromise between resolving the curvature of the pattern transition line and maintaining reasonable computation time. The agreement between the approximations and simulations is quite good, suggesting that the approximations capture the relevant aspects of spatial-pattern formation.

pattern. This is a key advantage of our approach because doing so by simulation alone is tedious and computationally intensive.

Discussion

Direct empirical evidence for tree-tree competition comes primarily from savannas known to be water limited, namely, those with <650 mm MAP (table 1). This suggests that tree-tree competition may limit tree density in such savannas, with the strength of competition (δ) likely increasing with water limitation. Here, we have shown that short-distance competitive effects of adult trees on juveniles, either by themselves or in combination with fire, can have powerful consequences for both the tree-grass balance in savannas and the formation of tree spatial pattern. Competition, acting individually, exerts a strong negative effect on density, and even relatively weak (small δ) competition can reduce tree density considerably. These results suggest that competition may be a key process limiting tree cover in arid and semiarid savannas and that it might still play a role in mesic savannas, where trees are only somewhat water limited (Sankaran et al. 2005, 2008; Bucini and Hanan 2007) and weak competition might be expected.

As competition is a density-dependent process, it cannot by itself drive tree extinction. Indeed, our simulation results suggest that tree density approaches a lower limit of $\rho^s[1] \approx 0.1095$ as competition strength becomes large. In contrast, the MFA and MSPA both predict that stationary tree density decays to 0 with increasing competition intensity. This discrepancy arises primarily because the MFA and MSPA summarize local interactions by approximating the expected number of tree-occupied neighbors around a grass-occupied site. When trees are sparsely distributed across the lattice and competition is strong, these average local densities do not adequately represent the very heterogeneous local neighborhood conditions that occur, and consequently both the MFA and MSPA overestimate the effects of competition (see app. B for further details). However, we note that even if the full distribution of neighborhood conditions is incorporated, there could still be discrepancies between simulations and the MFA and MSPA because of long-distance correlations that the approximations do not account for (see fig. 4*C*). The lower density limit observed in the simulations is greater than that seen in the driest savannas ($\rho^s[1] < 0.01$; Sankaran et al. 2005), implying that short-distance tree-tree competition alone cannot explain the full range of densities observed in water-limited savannas. We have assumed here that *b*, the tree reproductive rate, is fixed and that only competition and fire reduce density from the upper limit set by *b*. As fire is rare in very dry savannas because of the low grass biomass they support, this suggests that, in addition to competition, *b* must decrease for the model to be consistent with such low tree densities. Reduced seed set or increased failure of seeds to germinate at very low MAP could account for this decrease.

In isolation, fire acts in an all-or-nothing manner in our model and can affect both the density and the spatial structure of the tree population. In extreme scenarios, our results agree with recent studies suggesting that fire is capable of driving a transition from tree-grass coexistence to a grass-only state (fig. 2; eq. [9]; D'Odorico et al. 2006; Hanan et al. 2008). On the other hand, when σ is not near σ_c, our results are also in accord with studies suggesting that fire might not strongly regulate tree density (fig. 2; Menaut et al. 1990; Hochberg et al. 1994; Higgins et al. 2007).

We have shown that fire interacts with establishment competition in a nonlinear way that can strongly constrain tree density (fig. 3). This occurs in our model because (1) fire frequency increases with grass cover and (2) competition depresses tree density, thus increasing grass cover and the negative effects of fire. Combining competition with fire therefore leads to more frequent fire, which fur-

ther reduces tree density and increases grass cover. The result of this interaction is a reduction in tree density larger than that predicted by the sum of the independent effects of competition and fire for the same parameter values.

In general, fire will have its greatest effect on tree density when it is combined with competition of weak to intermediate strength (fig. 3; app. C). This is, to our knowledge, a novel result in the savanna literature, and it may have important implications for savanna ecology. For example, in semiarid and mesic savannas where competition and fire co-occur, their interaction could be a significant determinant of tree cover even if the individual influence of each factor would be relatively weak. Recent empirical studies have noted that the effect of fire on tree cover for a given mean annual precipitation is highly variable among savannas (Sankaran et al. 2005; Bucini and Hanan 2007; Higgins et al. 2007). Our results demonstrate that the interaction between tree-tree competition and fire can govern the magnitude of fire's effect on tree density. Taken together, these observations suggest that competition, which may vary in intensity, depending on soil moisture, soil type, tree species identity, and other factors, may be a missing ingredient in understanding the variable effects of fire on savanna tree density.

Empirical studies based on point pattern statistics have found tree distributions in a range of savannas to be regular, random, or clumped at short distances, generally clumped at intermediate scales, and clumped to random at larger scales (Skarpe 1991; Barot et al. 1999; Jeltsch et al. 1999; Caylor et al. 2003). Our approach allows us to derive the same type of spatial statistics used in these studies directly from our model, a key advantage relative to existing simulation-based analyses. We find that our model is capable of generating a similar range of patterns, suggesting that a small set of simple processes might account for much of the variation in spatial pattern among savannas. At the near-neighborhood scale, competition, acting singly, quickly overcomes the clustering driven by spatially limited dispersal and leads to regular spacing as competition strength increases (fig. 1*B*). At the far-neighborhood scale, spatial pattern is always at least weakly clustered, with the degree of clustering increasing with competition intensity (fig. 1*B*). Over longer distances, spatial pattern decays toward randomness, although clustering may persist at relatively large scales if the model is near a critical threshold for tree persistence (fig. 4*C*; Hiebeler 2005).

Our analytical approximation of the spatial-pattern transition line (eq. [10]) is an important result that links variation in model parameters to qualitative changes in the near-neighborhood spatial pattern. For fixed competition intensity, increasing the fire frequency past a critical level leads to a transition from regular tree spacing to clustering at the near-neighborhood scale (fig. 5; eq. [10]). This means that fire is capable of overcoming the regular dispersion driven by competition, even when competition is strong. Because the presence of competition is usually inferred from regular tree spacing in empirical studies (Gutiérrez and Fuentes 1979; Scholes and Archer 1997), competition's importance in fire-prone savannas may be largely underestimated.

Fire has been observed to promote tree clustering in savannas (Barot et al. 1999; Kennedy and Potgieter 2003). Although several theoretical studies have suggested that this pattern results from fire affecting isolated trees more than those protected by nearby trees (Menaut et al. 1990; Hochberg et al. 1994; Jeltsch et al. 1996), there is as yet relatively little direct, stem-level empirical evidence demonstrating such a protection effect (but see Holdo 2005). Our minimalistic treatment of fire, which does not include a protection effect, also leads to fire-driven tree clustering. To explain this effect, we focus on a tree-occupied site i. As the frequency of fire increases, the establishment probability decreases in both the near and far neighborhoods of site i, which reduces the density of trees in site i's far neighborhood. Because competition is dependent on local density, lower tree density in site i's far neighborhood means less competition and improved establishment chances for seeds dispersed into site i's near neighborhood. The average effect across the lattice is a relative increase in near-neighborhood density with increasing fire and a concomitant increase in near-neighborhood clustering. A similar effect has been noted by Hernández-García and López (2004) in a related spatial population model. Our results therefore suggest that an underlying tendency for fire to drive clustering may exist independent of a protection effect. Thus, while protection will clearly act to strengthen this tendency, it may not be the only means by which fire can promote tree clustering in savannas.

The persistent clustering at the far-neighborhood scale in our model is driven largely by dispersal-mediated facilitation. Ellner (2001) has shown that letting the far-neighborhood size go to infinity in a related MSPA model implies that $\rho_f[11] = \rho^2[1]$ and therefore that $g_f = 1$, a result that also holds for our model. Thus, in the global dispersal limit, the far-neighborhood scale clustering observed in figure 4 will disappear. The clustering observed at intermediate distances in some empirical spatial analyses (Skarpe 1991; Barot et al. 1999; Jeltsch et al. 1999; Caylor et al. 2003) is therefore consistent with dispersal-mediated facilitation. This form of facilitation does not, however, have strong effects on density in our model. To see this, consider that the MFA will have exactly the same form if we hold b constant and define $z_f = L^2 - (z_n + 1)$ and $\beta = b/(z_n + z_f) = b/(L^2 - 1)$, where L is the number of sites per side on the lattice. This substitution makes the per-site birth rate β contributed by each adult tree very

small while making the number of sites over which seeds are dispersed very large (i.e., the whole lattice). As the birth term of the MFA is the product of these two components, $\beta(z_n + z_f) = b$, its value is unaffected by this substitution. This suggests that allowing global dispersal will not have a major effect on $\rho^s[1]$. However, there might be some discrepancy between this mean-field result and numerical simulations at varying dispersal neighborhood size. We expect that such discrepancies will generally be small.

In contrast to our focus on competition, Scanlon et al. (2007) recently argued that observed large-scale power-law clustering in Kalahari tree distributions could be explained by a particularly strong form of local facilitation. While, as we have shown, facilitation is likely important for certain aspects of spatial-pattern formation, we do not find their singular focus on facilitation entirely convincing. First, tree density is a given in their model, not a result of tree population processes. Second, the reliability of the power-law pattern on which their inferences are based is unknown because they did not quantify the accuracy of their remotely sensed data set via standard ground-truthing techniques (e.g., Campbell 2006). Finally, empirical studies from other sites within the Kalahari region have shown clear evidence of tree-tree competition and the short-distance regular spacing it can promote (table 1).

Our core qualitative results, including the generally negative effect of competition, the all-or-nothing effect of fire, and nonlinear interaction between competition and fire, are not sensitive to the particular functional forms for competition and fire in our model. For example, many of the analytical results are based on a linear approximation of the exponential competition function used in the simulations and numerical results (see app. C). Although this substitution has quantitative consequences when δ is not near 0, the above-mentioned qualitative results are robust to it. Similarly, the all-or-nothing effects of fire hold when a linear, a hyperbolic (Michaelis-Menten), or a sigmoidal probability of fire curve is assumed (results not shown). Finally, the presence of a nonlinear interaction between fire and competition, with a peak in the $\Delta\rho^s[1]$ curve at low to intermediate competition intensities, occurs for all combinations of the different P_C^{Surv} and P_F^{Surv} functional forms mentioned above (results not shown). In contrast, the shapes of the responses of $\rho^s[1]$ to variation in δ (fig. 1) and σ (fig. 2) do depend on the functional forms of P_C^{Surv} and P_F^{Surv}.

The cost of our focus on tractability is that we have had to exclude factors that may be important in some savannas. These omissions suggest a few promising lines of future research. For example, variability in rainfall over time, and thus in demographic parameters, is an important feature of many water-limited savannas (Higgins et al. 2000). In a companion study, F. Vazquez, C. López, J. M. Calabrese, and M. A. Muñoz (unpublished manuscript) are exploring an extension of our model that incorporates stochastically varying rainfall. Going still farther, F. S. Bacelar, J. M. Calabrese, V. Grimm, and E. Hernández-García (unpublished manuscript) are extending our work by combining our model with a spatially explicit fire model to examine how spatial heterogeneity in fire spread affects savanna tree dynamics and spatial structure.

Our minimalistic and analytically tractable approach has yielded new insights about the interplay between competitive effects and fire on the density and spatial pattern of savanna tree populations. Tree-tree establishment competition, particularly in concert with fire, can strongly depress tree populations. Although competition's effect can be enhanced substantially when it occurs with fire, it is precisely these conditions that make competition harder to detect by traditional spatial-pattern analyses. Our results therefore suggest that the role of competition in structuring savanna tree populations, particularly in situations where relatively weak competition co-occurs with fire, has been largely underappreciated.

Acknowledgments

We thank F. Bacelar, R. Zinck, and two anonymous reviewers for helpful comments on the manuscript, and F. Jeltsch, S. Lautenbach, and T. Mueller for enlightening discussions. We are also grateful to F. Bacelar for kindly assisting with the robustness analysis of fire functional forms. This work was funded by the European Union project PATRES (pattern resilience; project NEST 43268).

APPENDIX A

Simulation Algorithm and Source Code

The two critical events that occur in the model are tree birth and death. Both types of events happen at constant rates, and the occurrence of birth and death events are independent of each other and of neighborhood conditions. In contrast, note that establishment, given that a birth event has occurred, depends explicitly on neighborhood conditions, as described below. The waiting times (or, equivalently, interarrival times) between births and deaths are therefore exponentially distributed and are characterized by the reciprocals of the birth (b) and death (α) rates, respectively. To simulate the model, we employ a waiting-time algorithm and choose exponentially distributed random numbers to jump directly from one birth or death event to the next (Bolker 2008).

To focus first on birth, at any point in time, each of N

currently living trees randomly selects one time to next birth from the exponential waiting-time distribution for births. The minimum of the N random draws is the time to the next birth event. The minimum of N independent and identically distributed random variables is known as the first order statistic (Ross 2000). In the case of the exponential distribution, the distribution of the first order statistic is also exponential, with parameter λN, where λ is the rate parameter of the original distribution (Ross 2000). Thus, instead of randomly selecting N times to next birth and then taking the minimum, we use the equivalent but more efficient method of drawing a single random variate from the distribution of the first order statistic. An equivalent procedure is performed to obtain the time to next death. The minimum of these two times defines both the time to the next event and whether that event represents a birth or death. Because the model is a Markov chain and therefore memory-less (i.e., the age of individual trees does not matter), the event (birth or death) is randomly assigned to an individual tree, and the appropriate procedures are implemented. The algorithm can be summarized as follows:

1. Initialize the lattice by randomly assigning N_{int} sites to state 1, set the value of the time counter to 0, and define the maximum time for which the simulation will run.
2. Obtain the time to next event and the identity (birth or death) of that event as described above.
3. If the event is a death, randomly select a tree-occupied site (1) and change it to a grass-occupied site (0).
4. If the event is a birth, randomly select a tree-occupied site, and then randomly select a birth site within the focal site's birth neighborhood. If the birth site is already occupied by a tree, do nothing. If the birth site is grass occupied, calculate the probability of surviving fire $P_{\text{F}}^{\text{Surv}}$, given current grass cover, using equation (2), and draw a Bernoulli random variable with probability of success $P_{\text{F}}^{\text{Surv}}$. If the new tree survives fire, scan the near (competition) neighborhood of the birth site, and count the number of adult trees (S). Calculate the probability of surviving competition as $P_{\text{C}}^{\text{Surv}} = e^{-\delta S}$, and draw another Bernoulli random variable. If the new individual survives to this point, establishment occurs, and the state of the birth site is changed from 0 to 1.
5. Add the event time to the time counter.
6. Repeat steps 2–5 until the value of the time counter exceeds the maximum time.

A Mathematica 6.0 implementation of the model can be found in the online edition of the *American Naturalist*. Code that appears in the *American Naturalist* has not been peer-reviewed, nor does the journal provide support.

APPENDIX B

Derivation of Mean-Field and Pair Approximations

Here, we provide derivations of both the mean-field and the multiscale pair approximations to the stochastic cellular-automaton savanna model described in the main text. We use the moment closure approach for continuous-time lattice models with multiple interaction scales described by Ellner (2001).

We wish to find a balance equation for $\rho[1]$ that has the general form

$$\frac{d\rho[1]}{dt} = \text{total birth rate} - \text{total death rate}. \tag{B1}$$

The rate of transition of a site in state 0 (grass occupied) to a site in state 1 (tree occupied) is governed by the density of trees in the birth neighborhood of the focal site; the probability of establishment, given the density of trees in the competition neighborhood of the focal site; and the probability of fire as a function of total grass cover. We consider these processes in turn. The birth neighborhood spans both near and far interaction neighborhoods. Since we have assumed that the per-site birth rate is the same in both the near and far portions of the birth neighborhood, the total contribution of the two neighborhoods to the birth rate of an unoccupied site can be written as

$$\beta(z_{\text{n}}q_{\text{n}}[1|0] + z_{\text{f}}q_{\text{f}}[1|0]), \tag{B2}$$

where $q_{\text{n}}[1|0]$ and $q_{\text{f}}[1|0]$ are, respectively, the near- and far-neighborhood local densities described in "Analytical Approximations." The total potential birth rate is obtained by multiplying equation (B2) by the global proportion of sites in state 0:

$$\beta(z_{\text{n}}q_{\text{n}}[1|0] + z_{\text{f}}q_{\text{f}}[1|0])(1 - \rho[1]). \tag{B3}$$

Because of the negative effects of nearby adults and fire on a seed's probability of establishment (P_E), the total potential birth rate must be appropriately discounted. Because we have defined both establishment competition and fire on a per–birth event basis, the per-birth probability of these events happening in the simulation model translates directly into the expected proportion of successful births, or

$$\beta(z_n q_n[1|0] + z_f q_f[1|0])P_E(1 - \rho[1]), \tag{B4}$$

where $P_E = P_C^{Surv} P_F^{Surv}$.

The probability of a new seedling surviving competition with already established adult neighbors depends on the density of adults in its competition neighborhood. Because the competition neighborhood covers only the near neighborhood, the expected local density of competitors is given by $q_n[1|0]$. The probability of surviving competition, which decays exponentially with the local density, can therefore be written as

$$P_C^{Surv} = e^{-\delta z_n q_n[1|0]}, \tag{B5}$$

where $z_n q_n[1|0]$ is the expected number of competitors and δ is the competition coefficient. The probability of surviving fire depends only on the global density of grass ($\rho[0] = 1 - \rho[1]$) and not on spatial position and is therefore simply equation (2). Combining the above, we can the write the total birth rate as

$$\beta(z_n q_n[1|0] + z_f q_f[1|0])e^{-\delta z_n q_n[1|0]} \frac{\sigma}{\sigma + 1 - \rho[1]}(1 - \rho[1]). \tag{B6}$$

As death of adult trees does not depend on local conditions and since we have implicitly rescaled time by setting $\alpha = 1$, the total death rate is simply $\rho[1]$. Equation (3) is obtained by substituting this death rate and equation (B6) into equation (B1).

The multiscale pair approximation is obtained from equation (3) by deriving equations for the pair frequencies in both the near and far neighborhoods and then expressing the local densities in equation (3) in terms of the singlet and pair frequencies. In doing so, we obtain an approximate system of moment equations that is closed to second order. Considering that there are two interaction neighborhoods, there are eight possible pair frequencies, which must obey the following constraints (Ellner 2001):

$$\begin{aligned} \sum \rho_n[ij] &= \sum \rho_f[ij] = 1, \\ \rho_n[10] &= \rho_n[01], \\ \rho_f[10] &= \rho_f[01], \\ \rho_n[00] + \rho_n[01] &= \rho_f[00] + \rho_f[01] = \rho[0]. \end{aligned} \tag{B7}$$

Therefore, only three frequencies are independent, and we retain $\rho[1]$, $\rho_n[11]$, and $\rho_f[11]$. Using equation (B7) and the definition of conditional probability, we can now express the local densities in terms of pair and singlet frequencies:

$$\begin{aligned} q_n[1|0] &= \frac{\rho_n[10]}{\rho[0]} = \frac{\rho[1] - \rho_n[11]}{1 - \rho[1]}, \\ q_f[1|0] &= \frac{\rho_f[10]}{\rho[0]} = \frac{\rho[1] - \rho_f[11]}{1 - \rho[1]}. \end{aligned} \tag{B8}$$

We now turn our attention to deriving equations for the pair frequencies in the near ($\rho_n[11]$) and far ($\rho_f[11]$) neighborhoods. To focus first on the near neighborhood, a pair of sites in either state 10 or 01 transitions to a 11 pair, depending on the birth contributions from both the near and far neighborhoods surrounding the unoccupied member of the pair, or

$$\beta[1 + (z_n - 1)q_n[1|0] + z_f q_f[1|0]]. \tag{B9}$$

The 1 inside the brackets accounts for the fact that we know there is at least one occupied site in the near neighborhood (because we are focusing on a 10 near-neighborhood pair), and the term $(z_n - 1)q_n[1|0]$ is approximately the expected number of occupied neighbors in the remaining near-neighborhood sites. It is approximate because it ignores the information that we know there is at least one neighbor; that is, it assumes that $q_n[1|01] = q_n[1|0]$. The exact term would depend on the triplet frequency $\rho_n[111]$, which in turn would depend on higher-order frequencies. As before, we must consider the reduction in the effective birth rate due to the negative effects of both establishment competition and fire. Neighborhood competition depends only on the near neighborhood, and thus we must take into account the knowledge that there is at least one occupied neighbor and the chance that there are others. Again using the pair approximation, we have

$$P_C^{\text{Surv}} = e^{-\delta[1+(z_n-1)q_n[1|0]]}. \tag{B10}$$

Because it does not depend on spatial position, the fire term is the same as before. Combining equations (2), (B9), and (B10), multiplying the resulting expression by the frequency of either 10 or 01 pairs (since these frequencies are equivalent), and accounting for the fact that there are two possible ways the transition can happen (i.e., from either a 10 or a 01 pair), the total pair formation rate is

$$2\beta[1 + (z_n - 1)q_n[1|0] + z_f q_f[1|0]]e^{-\delta[1+(z_n-1)q_n[1|0]]}\frac{\sigma}{\sigma + 1 - \rho[1]}\rho_n[10]\,. \tag{B11}$$

By the same logic, the total pair formation rate for the far neighborhood is

$$2\beta[z_n q_n[1|0] + 1 + (z_f - 1)q_f[1|0]]e^{-\delta z_n q_n[1|0]}\frac{\sigma}{\sigma + 1 - \rho[1]}\rho_f[10], \tag{B12}$$

where we have taken into account that in the far-neighborhood case, we know that one far-neighborhood site is occupied but do not know the status of the near neighborhood.

The transition from a 11 pair to either a 10 or a 01 pair depends only on the constant death rate, the frequency of 11 sites, and the fact that there are two ways this can happen. Therefore, in rescaled time ($\alpha = 1$), we have $2\rho_n[11]$ and $2\rho_f[11]$ for the near and far neighborhoods, respectively.

Combining equation (B11) and the appropriate pair loss rate, the pair equation for the near neighborhood is

$$\frac{1}{2}\frac{d\rho_n[11]}{dt} = \beta[1 + (z_n - 1)q_n[1|0] + z_f q_f[1|0]]e^{-\delta[1+(z_n-1)q_n[1|0]]}\frac{\sigma}{\sigma + 1 - \rho[1]}\rho_n[10] - \rho_n[11], \tag{B13}$$

and from equation (B12) and the corresponding loss rate, the pair density in the far neighborhood is

$$\frac{1}{2}\frac{d\rho_f[11]}{dt} = \beta[z_n q_n[1|0] + 1 + (z_f - 1)q_f[1|0]]e^{-\delta z_n q_n[1|0]}\frac{\sigma}{\sigma + 1 - \rho[1]}\rho_f[10] - \rho_f[11]. \tag{B14}$$

Finally, from the relationships in equation (B7), equations (3), (B13), and (B14), together define the coupled system given in equation (5).

We can continue in the same manner to derive a rate equation for the pair frequency in the neighborhood three cells away from a focal site ($\rho_3[11]$). Given that we have defined the dispersal neighborhood to cover the near and far neighborhoods, anything farther away (i.e., 3+ cells) cannot contribute to the gain term of the appropriate rate equation. Furthermore, we have no information about the occupancy status of the near and far neighborhoods. Combining these two facts, we see that the term representing the number of occupied neighbors around an empty site is the same as the corresponding term of equation (5a) for $\rho[1]$, or

$$\beta(z_n q_n[1|0] + z_f q_f[1|0]). \tag{B15}$$

The remaining steps are analogous to those above for the near and far neighborhoods and lead eventually to a rate equation for the $\rho_3[11]$ pair frequency:

$$\frac{1}{2}\frac{d\rho_3[11]}{dt} = \beta(z_n q_n[1|0] + z_f q_f[1|0])e^{-\delta z_n q_n[1|0]}\frac{\sigma}{\sigma + 1 - \rho[1]}\rho_3[10] - \rho_3[11]. \quad \text{(B16)}$$

Given that the same conditions hold for any neighborhood three cells away or farther, it is easy to verify that the pair frequency equations for these neighborhoods will all have the same form as equation (B16); thus, we may refer to the pair frequencies in any of these neighborhoods as $\rho_{3+}[11]$. Furthermore, the stationary solution of equation (B16) can numerically be shown to be $\rho_{3+}[11] = \rho^2[1]$, and thus the pair correlation statistic for neighborhoods three cells away and farther is $g_{3+} = \rho_{3+}[11]/\rho^2[1] = 1$. In other words, short-range seed dispersal makes sites at a distance of 3 cells or farther uncorrelated within the MSPA.

It is worth noting that Hiebeler (2005) has devised an alternative method for dealing with longer-distance correlations. His approach is to repeatedly apply the short-distance pair frequencies ($\rho_n[11]$ and $\rho_f[11]$ in our case) to approximate longer-distance pair frequencies. We have tried Hiebeler's method (results not shown) and found that it makes very little quantitative difference relative to the pure MSPA approach described above. The long-distance correlations observed in the simulations in figure 4*C* arise because the model is near a critical threshold (σ near σ_c; Hiebeler 2005). When this is the case, Hiebeler (2005) has shown that the method of repeatedly applying short-distance correlations to estimate longer-distance ones does not work well (see his fig. 5*B*). This, combined with the fact that Hiebeler's method introduces another layer of approximation, prompted us to retain the pure MSPA approach for calculating g_{3+}.

Finally, we note that the accuracy of our approximations will decrease as the strength of competition increases. The disagreement between the numerical simulations and our analytical approximations in the infinite-δ limit can be seen in figure 1*A*, where the value of $\rho^s[1]$ calculated from numerical simulations (*circles*) is approaching a constant value larger than 0 as δ increases, while the curves from the MFA and the MSPA decay to 0. The primary source of the discrepancy is the competition component of the establishment probability P_E when δ goes to infinity. In the numerical simulations, P_E can be larger than 0 for some of the grass-occupied sites even when $\delta \to \infty$; thus, new trees establish, and the system reaches a stationary density of trees larger than 0. However, in the mathematical approximation expressed in equation (3), as long as there are trees, $q_n[1|0] > 0$ and P_E becomes 0 for all sites (mean-field approach); thus, no new trees can establish, and $\rho[1]$ decays to 0.

To see this, consider a configuration with no fire and a few trees dispersed far from each other (low density) in a square lattice of side L. Given that the number of trees S in the near neighborhood of an empty site is either $S = 0$ in $L^2(1 - \rho[1])$ sites (empty regions) or $S = 1$ in $L^2\rho[1]$ sites (next to a tree), the establishment probability $P_E = \exp(-\delta S)$ as $\delta \to \infty$ is either $P_E = 1$ or $P_E = 0$, and its average value is $\langle P_E \rangle = 1 - \rho[1]$, which is close to 1 for small $\rho[1]$. However, in the mathematical approach expressed in equation (3), the establishment probability $P_E = \exp(-\delta z_n q_n[1|0])$ considers the average number of occupied sites next to an empty site, which is $z_n\langle q_n[1|0]\rangle = z_n * 0 * (1 - \rho[1]) + z_n * 1 * \rho[1] = z_n\rho[1]$, and because $\rho[1]$ is small but larger than 0, the average establishment probability in the large-δ limit is $P_E = \exp(-\delta z_n \rho[1]) = 0$.

One can also obtain an upper bound for the tree density if one realizes that, in the $\delta = \infty$ limit, the establishment probability is 0 for sites that belong to the near neighborhood of an occupied site. Therefore, the highest possible density of trees corresponds to a regular configuration where trees occupy every other site in both the horizontal and vertical directions on the lattice. Thus, the upper bound in tree density in the infinite-δ limit, as well as the maximum possible error between the simulations and analytical approximations, is 1/4.

APPENDIX C

Analysis of Mean-Field and Pair Approximation Equations

Mean Field

The evolution equation for the density of trees in the mean-field approximation (eq. [4]) can be written as

$$\frac{d\rho[1]}{dt} = be^{-\delta z_n \rho[1]} \frac{\sigma}{\sigma + 1 - \rho[1]} (\rho[1] - \rho^2[1]) - \rho[1]. \tag{C1}$$

This equation has two stationary solutions, with only one being stable for a given set of parameter values b, δ, and σ. The trivial solution, $\rho^0[1] = 0$, corresponds to a situation with no trees, while the second solution, $\rho^s[1] > 0$, represents a state of tree-grass coexistence. This positive solution is obtained by solving

$$b\sigma e^{-\delta z_n \rho^s[1]}(1 - \rho^s[1]) - \sigma - 1 + \rho^s[1] = 0. \tag{C2}$$

Since our work focuses mainly on the roles of competition and fire, b is typically fixed, and we vary the values of δ and σ. A transition from a tree-grass coexistence state ($0 < \rho^s[1] < 1$) to a treeless state ($\rho^s[1] = \rho^0[1] = 0$) occurs with decreasing σ (see fig. 2). An analytical approximation for $\rho^s[1]$ can be obtained close to the transition, or critical, point (i.e., for small $\rho[1]$) and for $\delta \ll 1$. Dropping terms involving $\rho^2[1]$ and expanding the exponential term to first order in $\rho[1]$, the solution of equation (C2) is equation (8).

We can obtain a better approximation for the stationary value of $\rho[1]$ farther away from the transition point (but still for $\delta \ll 1$) by doing as above but retaining terms involving $\rho^2[1]$. This results in a quadratic equation in $\rho[1]$ whose positive solution is

$$\rho^s[1] = \frac{b\sigma(1 + \delta z_n) - 1 - \sqrt{[b\sigma(1 + \delta z_n) - 1]^2 - 4b\sigma\delta z_n[(b - 1)\sigma - 1]}}{2b\sigma\delta z_n}. \tag{C3}$$

We now focus on the combined effects of competition and fire. To maintain tractability, we base our analysis on equation (8). The effect of competition alone is obtained by taking the limit of equation (8) as $\sigma \to \infty$, which is

$$\rho^s[1] = \frac{b - 1}{b(\delta z_n + 1)}. \tag{C4}$$

Subtracting equation (8) from equation (C4) and simplifying yields the difference in stationary tree density ($\Delta\rho^s[1]$) between the competition-only case (eq. [C4]) and cases where competition is combined with fire (eq. [8]):

$$\Delta\rho^s[1] = \frac{1 + b\delta z_n}{b(1 + \delta z_n)[b\sigma(1 + \delta z_n) - 1]}. \tag{C5}$$

When $\delta = 0$, this difference reduces to $1/b(b\sigma - 1)$, and in the limit where $\delta \to \infty$, $\Delta\rho^s[1] = 0$. To find the maximum of this curve, we differentiate equation (C5) with respect to δ, resulting in

$$\frac{d\rho^s[1]}{d\delta} = \frac{z_n(1 - b\{1 + (\delta z_n + 1)[2 + b(\delta z_n - 1)]\sigma\})}{b(\delta z_n + 1)^2[b\sigma(\delta z_n + 1) - 1]^2}. \tag{C6}$$

Setting equation (C6) to 0 and solving for δ yields

$$\delta_m = \frac{-\sigma + \sqrt{\sigma(b - 1)[\sigma(b - 1) - 1]}}{bz_n\sigma}. \tag{C7}$$

For fixed b, this peak moves to the right (toward larger δ values) as σ increases, approaching $\delta_m = (b - 2)/bz_n$ as $\sigma \to \infty$. As σ decreases, the peak moves to the left until it meets the Y-axis ($\delta = 0$) when σ equals a critical lower value. Setting equation (C7) equal to 0 and solving for σ, we obtain this critical value of σ at which the interior maximum of the $\Delta\rho^s[1]$ curve observed in figure 3 disappears:

$$\sigma_m = \frac{b - 1}{b(b - 2)}. \tag{C8}$$

As σ_m is generally very close to σ_c (i.e., very close to the point at which the tree population becomes extinct), this analysis suggests that the $\Delta\rho^s[1]$ curve will generally have an interior peak at small to intermediate values of the competition parameter, as observed in figure 3.

Pair Approximation

As spatial pattern in the model is most variable at the near-neighborhood scale, we focus our analysis of the pair approximation at this scale. Our goal is to obtain an approximate expression for the pattern transition line $\hat{\sigma}(\delta)$, along which $g_n = 1$ in the $(\hat{\sigma}, \delta)$ plane. This line separates the plane into a region where clustering occurs ($g_n > 1$) and a region where regular dispersion ($g_n < 1$) occurs. We obtain this pattern transition line by considering the system of equations (5) in a particular stationary state in which the relation $\rho_n[11] = \rho^2[1] = \text{constant}$ ($g_n = 1$) holds and by solving for $\hat{\sigma}$ as a function of δ. The process used to obtain this expression is involved and requires several approximations to remain tractable. These steps are detailed below.

To simplify our analysis, we start by performing the following change of variables:

$$q_n[1|0] = \frac{\rho[1] - \rho_n[11]}{1 - \rho[1]},$$
$$q_f[1|0] = \frac{\rho[1] - \rho_f[11]}{1 - \rho[1]}. \tag{C9}$$

We then rewrite equations (5b) and (5c) in terms of these variables. We obtain, in the stationary state,

$$\frac{-1}{2}\frac{dq_n[1|0]}{dt} = A[1 + (z_n - 1)q_n[1|0] + z_f q_f[1|0]]e^{-\delta[1+(z_n-1)q_n[1|0]]}q_n[1|0] + q_n[1|0] - C = 0, \tag{C10}$$

$$\frac{-1}{2}\frac{dq_f[1|0]}{dt} = A(1 + z_n q_n[1|0] + z_f q_f[1|0])e^{-\delta z_n q_n[1|0]}q_f[1|0] + q_f[1|0] - C = 0, \tag{C11}$$

where we have defined

$$A \equiv \frac{\beta\sigma}{\sigma + 1 - \rho[1]},$$
$$C \equiv \frac{\rho[1]}{1 - \rho[1]}. \tag{C12}$$

To analyze the above equations on the $g_n = 1$ line, we note that $q_n[1|0] = \rho[1]$, given that $\rho_n[11] = \rho^2[1]$ for $g_n = 1$. Then, equation (C10) becomes

$$A[1 + (z_n - 1)\rho[1] + z_f q_f[1|0]]e^{-\delta[1+(z_n-1)\rho[1]]}\rho[1] + \rho[1] - C = 0. \tag{C13}$$

Figure 5 shows that for large enough δ, the transition from clustering to regular spacing happens for values of σ very close to the critical value σ_c, where $\rho[1]$ is small. Then, given that $q_f[1|0]$ is smaller than $\rho[1]$, we consider $q_f[1|0] \ll 1$ and expand equation (C11) to first order in $q_f[1|0]$ and zeroth order in $q_n[1|0]$. We obtain

$$(A + 1)q_f[1|0] - C = 0. \tag{C14}$$

For $\rho[1] \ll 1$,

$$A \approx \frac{\beta\sigma}{\sigma + 1} + \frac{\beta\sigma\rho[1]}{(\sigma + 1)^2} = a_0 + a_1\rho[1],$$

and $C \approx \rho[1](1 + \rho[1])$. Then, to first order in $\rho[1]$, we obtain

$$q_f[1|0] \approx \frac{(\sigma + 1)\rho[1]}{1 + \sigma(\beta + 1)} = y\rho[1]. \tag{C15}$$

Now, replacing the above expression for $q_f[1|0]$ in equation (C13) and expanding to second order in $\rho[1]$, we obtain

$$\rho[1]\left(e^{-\delta}a_0 + \{e^{-\delta}a_0[(z_n - 1)(1 - \delta) + z_f y] + e^{-\delta}a_1 - 1\}\rho[1]\right) = 0. \tag{C16}$$

Taking advantage of the close correspondence between the stationary-state densities in the mean-field and pair approximations, we take the solution $\rho^s[1] > 0$ (eq. [8]) and arrive at the following equation that relates σ and δ on the $g_n = 1$ line:

$$e^{-\delta}a_0[1 - b\sigma(1 + \delta z_n)] + \{e^{-\delta}a_0[(z_n - 1)(1 - \delta) + z_f y] + e^{-\delta}a_1 - 1\}[1 + (1 - b)\sigma] = 0. \tag{C17}$$

Substituting the expressions for a_0, a_1, and y into the above equation leads to a fourth-order polynomial in σ. To simplify the calculations, we use the fact that our analysis is for σ close to σ_c, so that $\sigma - \sigma_c = \hat{\sigma} \ll 1$. We then make the substitution $\sigma = \hat{\sigma} + \sigma_c$ in the above-mentioned fourth-order polynomial, expand to first order in $\hat{\sigma}$, and solve for $\hat{\sigma}$, yielding equation (10).

APPENDIX D

Additional Results

In this appendix, we provide a set of figures analogous to those in the main text but for the case $b = 8$. As can be seen, all major qualitative results still hold, and the quantitative accuracy of the approximations is, in some cases, better. As the legends for the complementary figures in the main text apply, for the most part, here as well, we note only what has changed in these figures relative to those in the text.

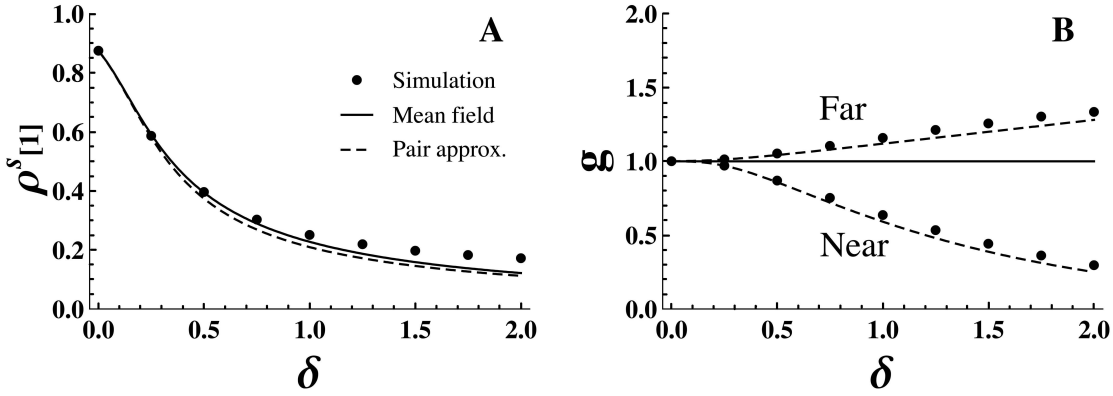

Figure D1: Same as figure 1 but for $b = 8$.

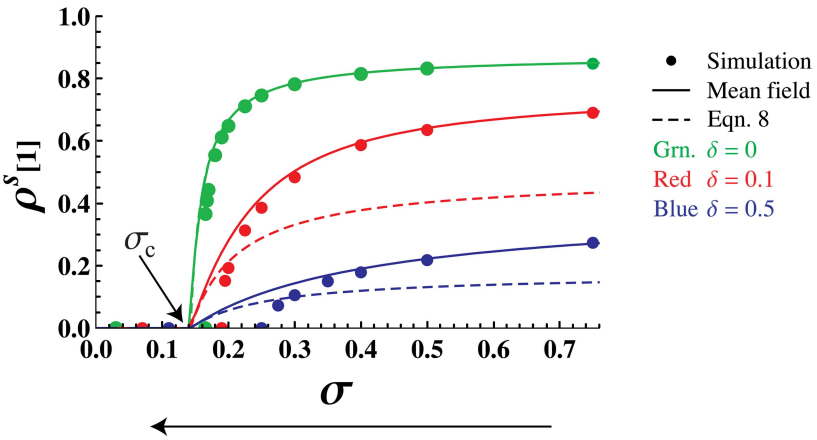

Figure D2: Same as figure 2 but for $b = 8$.

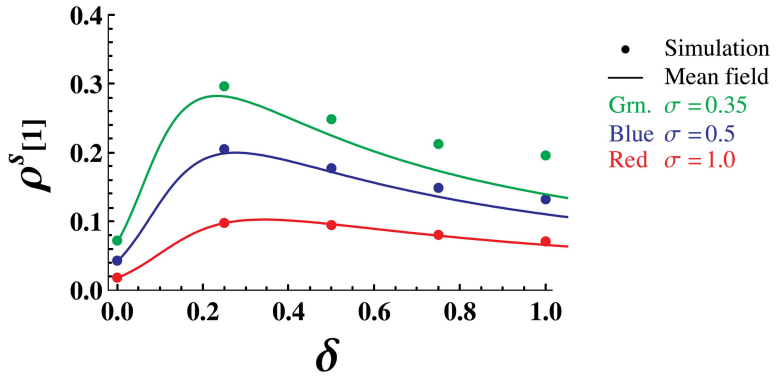

Figure D3: Same as figure 3 but for $b = 8$. In addition, the colors here refer to different levels of fire (*green*, high fire [$\sigma = 0.35$]; *blue*, medium fire [$\sigma = 0.5$]; and *red*, low fire [$\sigma = 1.0$]).

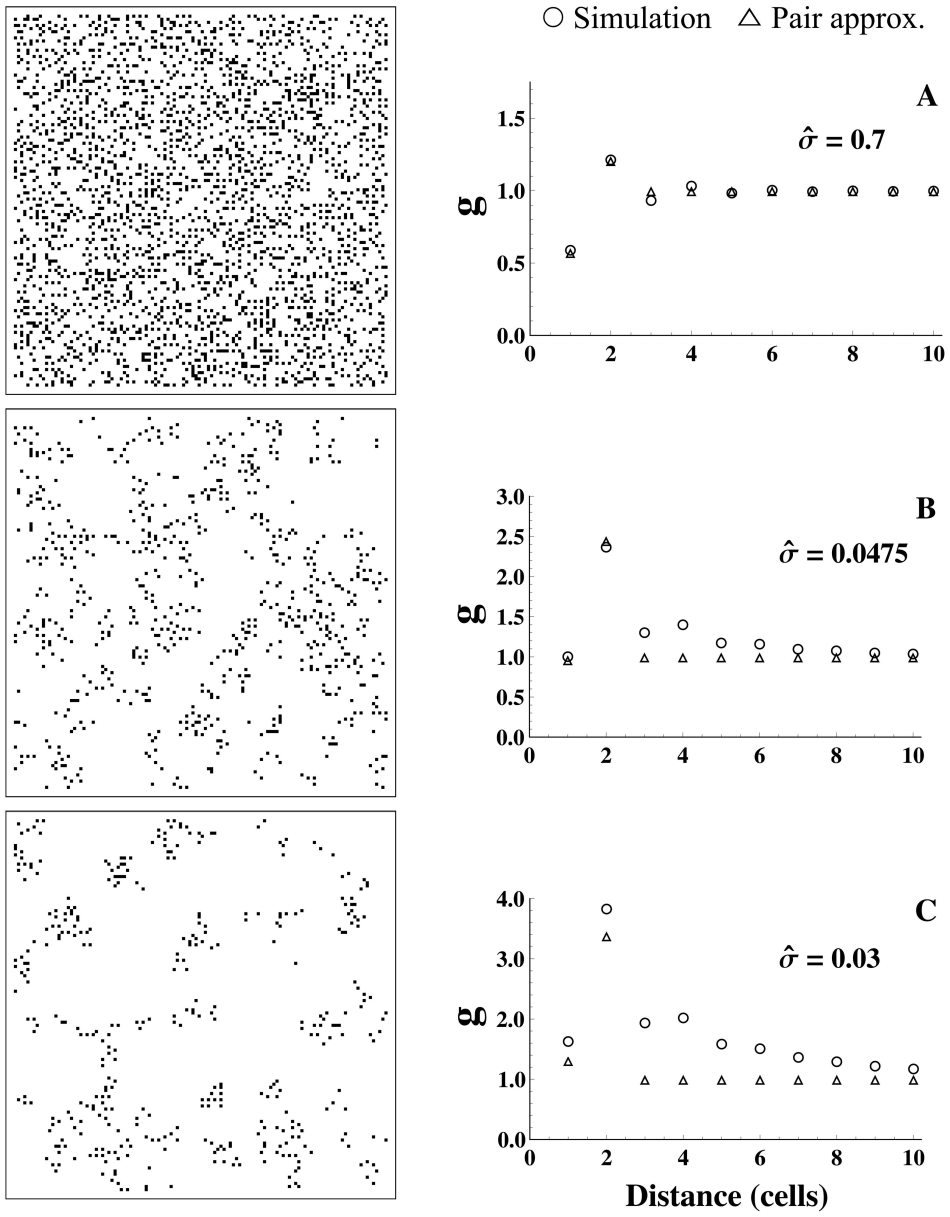

Figure D4: Same as figure 4 but for $b = 8$ and different values of the scaled fire parameter (*A*, $\hat{\sigma} = 0.7$; *B*, $\hat{\sigma} = 0.0475$; *C*, $\hat{\sigma} = 0.03$).

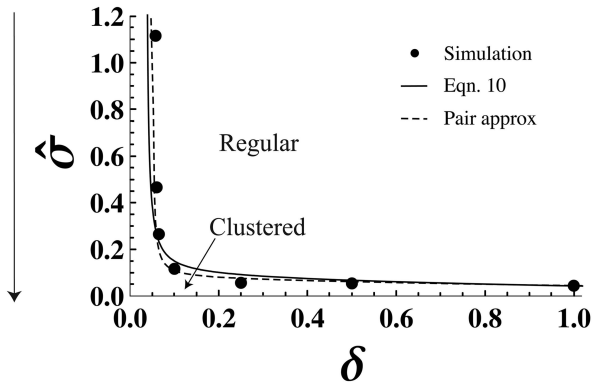

Figure D5: Same as figure 5 but for $b = 8$.

Literature Cited

Barot, S., J. Gignoux, and J.-C. Menaut. 1999. Demography of a savanna palm tree: predictions from comprehensive spatial pattern analyses. Ecology 80:1987–2005.

Baxter, P. W. J., and W. M. Getz. 2005. A model-framed evaluation of elephant effects on tree and fire dynamics in African savannas. Ecological Applications 15:1331–1341.

Belsky, A. J. 1994. Influences of trees on savanna productivity: tests of shade, nutrients, and tree-grass competition. Ecology 75:922–932.

Belsky, A. J., R. G. Amundson, J. M. Duxbury, S. J. Riha, A. R. Ali, and S. M. Mwonga. 1989. The effects of trees on their physical, chemical and biological environments in a semi-arid savanna in Kenya. Journal of Applied Ecology 26:1005–1024.

Belsky, A. J., S. M. Mwonga, R. G. Amundson, J. M. Duxbury, and A. R. Ali. 1993. Comparative effects of isolated trees on their undercanopy environments in high- and low-rainfall savannas. Journal of Applied Ecology 30:143–155.

Boaler, S. B., and K. C. Sciwale. 1966. Ecology of a Miombo site, Lupa North Forest Reserve, Tanzania. III. Effects on the vegetation of local cultivation practices. Journal of Ecology 54:577–587.

Bolker, B. M. 2008. Ecological models and data in R. Princeton University Press, Princeton, NJ.

Bolker, B. M., S. W. Pacala, and S. A. Levin. 2000. Moment methods for ecological processes in continuous space. Pages 388–411 *in* U. Dieckmann, R. Law, and J. A. J. Metz, eds. The geometry of ecological interactions: simplifying spatial complexity. Cambridge University Press, Cambridge.

Bond, W. J. 2008. What limits trees in C4 grasslands and savannas? Annual Review of Ecology, Evolution, and Systematics 39:641–659.

Bond, W. J., G. F. Midgley, and F. I. Woodward. 2003. What controls South African vegetation: climate or fire? South African Journal of Botany 69:79–91.

Bucini, G., and N. P. Hanan. 2007. A continental-scale analysis of tree cover in African savannas. Global Ecology and Biogeography 16:593–605.

Campbell, J. B. 2006. Introduction to remote sensing. 4th ed. Guilford, New York.

Casper, B. B., H. J. Schenk, and R. B. Jackson. 2003. Defining a plant's belowground zone of influence. Ecology 84:2313–2321.

Caylor, K. K., H. H. Shugart, P. R. Dowty, and T. M. Smith. 2003. Tree spacing along the Kalahari transect in southern Africa. Journal of Arid Environments 54:281–296.

D'Odorico, P., F. Laio, and L. Ridolfi. 2006. A probabilistic analysis of fire-induced tree-grass coexistence in savannas. American Naturalist 167:E79–E87.

Ellner, S. P. 2001. Pair approximation for lattice models with multiple interaction scales. Journal of Theoretical Biology 210:435–447.

Grimm, V., E. Revilla, U. Berger, F. Jeltsch, W. M. Mooij, S. F. Railsback, H. H. Thulke, J. Weiner, T. Wiegand, and D. L. DeAngelis. 2005. Pattern-oriented modeling of agent-based complex systems: lessons from ecology. Science 310:987–991.

Gutiérrez, J. R., and E. R. Fuentes. 1979. Evidence for intraspecific competition in the *Acacia caven* (leguminosae) savanna of Chile. Oecologia Plantarum 14:151–158.

Hanan, N. P., W. B. Sea, G. Dangelmayr, and N. Govender. 2008. Do fires in savannas consume woody biomass? a comment on approaches to modeling savanna dynamics. American Naturalist 171:851–856.

Hernández-García, E., and C. López. 2004. Clustering, advection, and patterns in a model of population dynamics with neighborhood-dependent rates. Physical Review E 70:016216.

Hiebeler, D. 2005. Spatially correlated disturbances in a locally dispersing population model. Journal of Theoretical Biology 232:143–149.

Higgins, S. I., W. J. Bond, and W. S. W. Trollope. 2000. Fire, resprouting and variability: a recipe for grass-tree coexistence in savanna. Journal of Ecology 88:213–229.

Higgins, S. I., W. J. Bond, E. C. February, A. Bronn, D. I. W. Euston-Brown, B. Enslin, N. Govender, et al. 2007. Effects of four decades of fire manipulation on woody vegetation structure in savanna. Ecology 88:1119–1125.

Hochberg, M. E., J. C. Menaut, and J. Gignoux. 1994. The influences of tree biology and fire in the spatial structure of the West African savannah. Journal of Ecology 82:217–226.

Holdo, R. M. 2005. Stem mortality following fire in Kalahari sand vegetation: effects of frost, prior damage, and tree neighbourhoods. Plant Ecology 180:77–86.

———. 2006. Elephant herbivory, frost damage and topkill in Kalahari sand woodland savanna trees. Journal of Vegetation Science 17:509–518.

Holdo, R. M., R. D. Holt, and J. M. Fryxell. 2009. Grazers, browsers, and fire influence the extent and spatial pattern of tree cover in the Serengeti. Ecological Applications 19:95–109.

Jeltsch, F., S. J. Milton, W. R. J. Dean, and N. van Rooyen. 1996. Tree spacing and coexistence in semiarid savannas. Journal of Ecology 84:583–595.

Jeltsch, F., S. J. Milton, W. R. J. Dean, N. van Rooyen, and K. A. Moloney. 1998. Modelling the impact of small-scale heterogeneities on tree-grass coexistence in semi-arid savannas. Journal of Ecology 86:780–793.

Jeltsch, F., K. Moloney, and S. J. Milton. 1999. Detecting process from snapshot pattern: lessons from tree spacing in the southern Kalahari. Oikos 85:451–466.

Jeltsch, F., G. E. Weber, and V. Grimm. 2000. Ecological buffering mechanisms in savannas: a unifying theory of long-term tree-grass coexistence. Plant Ecology 150:161–171.

Kennedy, A. D., and A. L. F. Potgieter. 2003. Fire season affects size and architecture of *Colophospermum mopane* in southern African savannas. Plant Ecology 167:179–192.

Marro, J., and R. Dickman. 1999. Nonequilibrium phase transitions in lattice models. Cambridge University Press, Cambridge.

Matsuda, H., N. Ogita, A. Sasaki, and K. Sato. 1992. Statistical mechanics of population: the lattice Lotka-Volterra model. Progress of Theoretical Physics 88:1035–1049.

Menaut, J. C., J. Gignoux, C. Prado, and J. Clobert. 1990. Tree community dynamics in a humid savanna of the Ivory Coast: modeling the effects of fire and competition with grass and neighbors. Journal of Biogeography 17:471–481.

Meyer, K. M., K. Wiegand, D. Ward, and A. Moustakas. 2007. SATCHMO: a spatial simulation model of growth, competition, and mortality in cycling savanna patches. Ecological Modelling 209:377–391.

Meyer, K. M., D. Ward, K. Wiegand, and A. Moustakas. 2008. Multiproxy evidence for competition between savanna woody species. Perspectives in Plant Ecology, Evolution, and Systematics 10:63–72.

Moustakas, A., M. Guenther, K. Wiegand, K.-H. Mueller, D. Ward, K. M. Meyer, and F. Jeltsch. 2006. Long-term mortality patterns of the deep-rooted *Acacia erioloba*: the middle class shall die! Journal of Vegetation Science 17:473–480.

Moustakas, A., K. Wiegand, S. Getzin, D. Ward, K. M. Meyer, M. Guenther, and K.-H. Mueller. 2008. Spacing patterns of an *Acacia* tree in the Kalahari over a 61-year period: how clumped becomes regular and vice versa. Acta Oecologica 33:355–364.

Neke, K. S., N. Owen-Smith, and E. T. F. Witkowski. 2006. Comparative resprouting response of savanna woody plant species following harvesting: the value of persistence. Forest Ecology and Management 232:114–123.

Pellew, R. A. P. 1983. The impacts of elephant, giraffe and fire upon the *Acacia tortilis* woodlands of the Serengeti. African Journal of Ecology 21:41–74.

Peterson, D. W., and P. B. Reich. 2001. Prescribed fire in oak savanna: fire frequency effects on stand structure and dynamics. Ecological Applications 11:914–927.

Ross, S. M. 2000. Introduction to probability models. 7th ed. Academic Press, San Diego, CA.

Sankaran, M., J. Ratnam, and N. P. Hanan. 2004. Tree-grass coexistence in savannas revisited: insights from an examination of assumptions and mechanisms invoked in existing models. Ecology Letters 7:480–490.

Sankaran, M., N. P. Hanan, R. J. Scholes, J. Ratnam, D. J. Augustine, B. S. Cade, J. Gignoux, et al. 2005. Determinants of woody cover in African savannas. Nature 438:846–849.

Sankaran, M., J. Ratnam, and N. Hanan. 2008. Woody cover in African savannas: the role of resources, fire and herbivory. Global Ecology and Biogeography 17:236–245.

Sarmiento, G. 1984. The ecology of Neotropical savannas. Harvard University Press, Cambridge, MA.

Scanlon, T. M., K. K. Caylor, S. A. Levin, and I. Rodriguez-Iturbe. 2007. Positive feedbacks promote power-law clustering of Kalahari vegetation. Nature 449:209–212.

Scheiter, S., and S. I. Higgins. 2007. Partitioning of root and shoot competition and the stability of savannas. American Naturalist 170: 587–601.

Schenk, H. J., and R. B. Jackson. 2002. Rooting depths, lateral root spreads and below-ground/above-ground allometries of plants in water-limited ecosystems. Journal of Ecology 90:480–494.

Scholes, R. J., and S. R. Archer. 1997. Tree-grass interactions in savannas. Annual Review of Ecology and Systematics 28:517–544.

Skarpe, C. 1991. Spatial patterns and dynamics of woody vegetation in an arid savanna. Journal of Vegetation Science 2:565–572.

Smith, T. M., and P. S. Goodman. 1986. The effect of competition on the structure and dynamics of *Acacia* savannas in southern Africa. Journal of Ecology 74:1031–1044.

Smith, T. M., and K. Grant. 1986. The role of competition in the spacing of trees in a *Burkea africana–Terminalia sericea* savanna. Biotropica 18:219–223.

Stanley, H. E. 1971. Introduction to phase transitions and critical phenomena. Oxford University Press, Oxford.

Stoyan, D., and H. Stoyan. 1994. Fractals, random shapes and point fields: methods of geometrical statistics. Wiley, Chichester.

Tybirk, K., L. H. Schmidt, and T. Hauser. 1994. Notes on soil seed banks of African acacias. African Journal of Ecology 32:327–330.

van Langevelde, F., C. van de Vijver, L. Kumar, J. van de Koppel, N. de Ridder, J. van Andel, A. K. Skidmore, et al. 2003. Effects of fire and herbivory on the stability of savanna ecosystems. Ecology 84: 337–350.

van Wilgen, B. W., H. C. Biggs, S. P. O'Regan, and N. Mare. 2000. A fire history of the savanna ecosystems in the Kruger National Park, South Africa, between 1941 and 1996. South African Journal of Science 96:167–183.

Walker, B. H., and I. Noy-Meir. 1982. Aspects of the stability and resilience of savanna ecosystems. Pages 556–590 *in* B. J. Huntley, and B. H. Walker, eds. Ecology of tropical savannas. Springer, Berlin.

Walker, B. H., D. Ludwig, C. S. Holling, and R. M. Peterman. 1981. Stability of semi-arid savanna grazing systems. Journal of Ecology 69:473–498.

Wiegand, K., D. Saitz, and D. Ward. 2006. A patch-dynamics approach to savanna dynamics and woody plant encroachment: insights from an arid savanna. Perspectives in Plant Ecology, Evolution, and Systematics 7:229–242.

Wiegand, T., and K. Moloney. 2004. Rings, circles, and null-models for point pattern analysis in ecology. Oikos 104:209–229.

Witkowski, E. T. F., and R. D. Garner. 2000. Spatial distribution of soil seed banks of three African savanna woody species at two contrasting sites. Plant Ecology 149:91–106.

Associate Editor: Christopher A. Klausmeier
Editor: Donald L. DeAngelis